Modelling and experimenting thermal energy storage through the use of PCM in low thermal inertia office

Duarte Pedro Vicente Drumond de Abreu
duarte.drumond@tecnico.ulisboa.pt

Instituto Superior Técnico, Universidade de Lisboa, Portugal

November 2018

Abstract

Within the scope of this thesis, thirty *DuPont Energain*® thermal mass boards were tested inside a shipping container located in Oeiras, Portugal. These phase change material (PCM) boards have a $21.7°C$ melting point and they were experimented during August (Summer) as internal mass due to a structure specifically designed for this project. Results showed that these latent heat storage systems induced an indoor peak temperatures shift of three hours and a slight indoor temperatures reduction. An *EnergyPlus*® model was validated using measured data and several parametric studies were made using this model. In this case, it was found that the best solution for this low thermal inertia enclosure was incorporating forty eight panels with $10\,mm$ of thickness and a melting point of $20°C$. Although these panels have a payback period of thirty two years, in the future it can fall into a more acceptable value of five years.

Keywords: Phase change material, Thermal inertia, Thermal energy storage systems, Buildings applications, *EnergyPlus*®

1. Introduction

Is the world spinning too fast? Large newspapers headers have been concerning world population but has it been enough to spark new habits on energy consumption? Some new studies on this matter say the opposite. Recent forecasts affirm that by 2050, energy consumption would have risen around 80% in respect to the value registered in 2010 of which more than 35% is due to space heating and cooling [1].

In this sense, an effort to discover reliable passive cooling/heating strategies that could take over the ones that use conventional sources of energy have been done. Thermal energy storage (TES) systems are among those and are divided into three main groups: (a) sensible heat storage, (b) latent heat storage and (c) thermochemical heat storage. TES systems are mainly latent heat storage systems since this type of thermal energy predominates over sensible and, thermochemical is at an early stage. In latent heat storage, the amount of heat stored, Q, depends on the mass of the material, m, the fraction of melted material, a_m, and the latent heat of fusion per unit of mass, Δh_m (Eq. 1) [2].

$$Q \approx m a_m \Delta h_m \,, \tag{1}$$

Latent heat storage systems are usually substances that absorb and release latent heat when a phase change occurs and, for this reason, they are called phase change materials (PCM).

In order to be effective latent heat thermal energy storage (LHTES) systems, PCM should satisfy several features. In terms of thermophysical properties, these materials must have high latent heat of fusion per unit of mass or volume, high thermal conductivity, no segregation, small volume change, high specific heat capacity, high volumetric mass density and a congruent melting. In terms of kinetic properties, although they should not suffer from supercooling, a high nucleation rate, a high rate of crystallization and a long term thermal stability are desirable. Moreover, chemically speaking, PCM should have complete reversible melt/freeze cycles, compatibility with constructions materials, no toxicity, no flammability and no corrosiveness. Lastly, these materials should be abundant, cost effective, recyclable and should not have an environmental impact's production [3, 4].

Furthermore, PCM can be classified according to their nature or phase change. The first classification split up PCM into eutectic, inorganic and organic (paraffin and non-paraffin), whereas the second separate them into solid-liquid, solid-solid, gas-solid and gas-liquid. Among those, the most widely studied and commonly applied in building's cooling and heating strategies are organic paraffin and solid liquid PCM [4, 5].

PCM can be integrated into buildings envelopes employing three main techniques such us incorporation (liquid or powdered PCM), immersion (liquid) and, the most commonly used, encapsulation [6]. Encapsulation categorization depends on capsule's diameter: nano-encapsulation ($\varnothing < 1\mu m$), micro-encapsulation ($1\mu m < \varnothing < 1mm$) and macro-encapsulation ($1mm < \varnothing < 1cm$) [7].

For the purpose of modelling PCM integrated in buildings, several software provide dedicated modules that simulate accurately PCM's behaviour. From these software, *EnergyPlus*® is one of those that already have a widely comprehensive list of modelled PCM, including DuPont Energain® thermal mass system [8–11], the PCM that will be studied in this work.

Moreover, experimental data of PCM should be measured and registered so as to validate the *EnergyPlus*® model. This validation process depends on two indexes: the normalised mean bias error (NMBE) and the coefficient of variation of the root mean square error (CVRMSE) [12]. It is said we have a validated model when the NMBE (Eq. 2) and CVRMSE (Eq. 3) values are within the range of ±10% and ±30% respectively. These indexes depend on the measured temperature, $y_{meas,i}$, predicted temperature, $y_{sim,i}$, mean hourly measured temperature, $\bar{y}_{meas}$, number of data points, n, and number of predictor variables, p.

$$NMBE = \frac{\sum_{i=1}^{n}(y_{sim,i} - y_{meas,i})}{\bar{y}_{measured} \times (n-p)} \quad (2)$$

$$CVRMSE = \frac{1}{\bar{y}_{meas}}\sqrt{\frac{\sum_{i=1}^{n}(y_{sim,i} - y_{meas,i})^2}{n-p-1}} \quad (3)$$

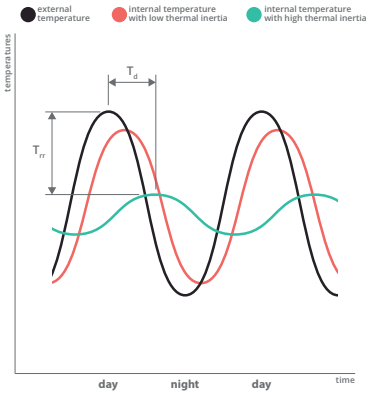

Figure 1: Stabilising effect of thermal inertia on internal temperature.

Nonetheless, integrating PCM into a building's envelope increases its thermal inertia. Besides increasing thermal comfort, this property can also induce peak temperatures delay, T_d, and temperatures range reduction, T_{rr}. The higher the thermal inertia, the higher the value of T_d and T_{rr}, which results in a stabilising effect of indoor temperatures (Fig. 1).

2. Implementation

2.1. Problem formulation

PCM *DuPont Energain*® thermal mass systems were installed into a shipping container whose dimensions are 6058 mm long, 2438 mm wide and 2591 mm high (Fig. 2).

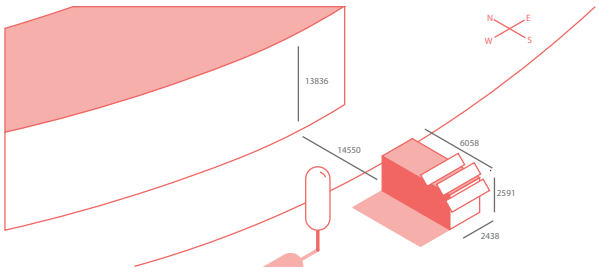

Figure 2: Schematic representation of the shipping container and its surroundings.

Although this container was made with corten steel, the West sided-wall had one 2 mm thickness layer of plasticized polyvinyl chloride (PVC-P), the East sided-wall and the South door had two 2 mm thickness layers of the same material and the floor had one extra 10 mm thickness layer of medium density fiberboard (MDF).

Thermal inertia, λ, tells us the capacity that each surface has to store heat per square meter for later release, whereas stored heat, Q, complements this info by specifying the amount of sensible heat stored into them. On the other hand, overall heat transfer coefficient, U, reveals the rate at which heat passes through each surface per square meter.

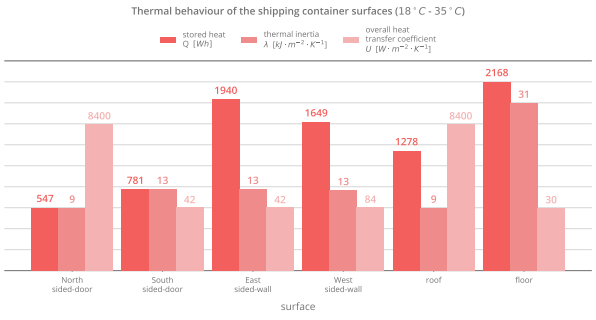

Figure 3: Thermal behaviour of the shipping container surfaces (18°C to 35°C).

Figure 3 shows us that this container was enclosured with low thermal inertia surfaces which did not insulate the inner space effectively from outside conditions. Therefore, overheating and overcooling temperatures are expected during

warmer and colder climates.

The shipping container was settled at Instituto Superior Técnico (Taguspark campus) which is located in Oeiras, Portugal. According to the Köppen-Geiger climate classification [13], this portuguese municipality belongs to an area characterized by a temperate weather with dry hot Summer. For this reason, its weather is classified as Csa.

Inside this low thermal inertia space, thirty *DuPont Energain*® thermal mass systems were installed. These PCM boards are made of a mixture of ethylene based polymer (40%) and paraffin wax (60%). The board is laminated on both sides with a $100\,\mu m$ thickness aluminium sheet and the edges are closed with a $75\,\mu m$ thickness aluminium tape. Sheltering the mixture with aluminium not only prevents from melted paraffin leakage, but also increases the thermal conductivity of the board which contributes to an improvement on the latent heat storage effectiveness. Each board is $5.2\,mm$ thick, $1000\,mm$ wide and $1198\,mm$ long. It weighs $5.391\,kg$ and has a volumetric mass density of $865.385\,kg \cdot m^{-2}$.

The paraffin wax is the PCM component of these boards and melts around $21.7°C$, whereas the solidification process starts when temperatures fall below $18°C$. The enthalpy vs temperatures curve of these boards was obtained from differential scanning calorimeter (DSC) measurements with a heating rate of $0.05°C \cdot min^{-1}$ [14] (Fig. 4).

Each board has a total heat storage capacity of $140\,kJ \cdot kg^{-1}$, half of which is due to latent heat storage.

2.2. Experimental set up

In order to incorporate thirty boards inside the shipping container anteriorly described, a totally new structure was designed within the scope of this thesis. In accordance with some trial *EnergyPlus*® simulations, the most suitable place to incorporate this structure was next to the ceiling owing to air stratification and the benefits it can bring to the amount of heat stored. This structure should take over the maximum width and length of the shipping container so that it can take in the highest PCM boards quantity possible. Furthermore, it had to allow take and put boards constantly and let enough space for a $1.90\,m$ high person walk freely and straight below the boards. All these constraints led to come up with a solution that was similar to a clearing tray system. The final wooden structure can be seen in figures 5 and 6.

Having the structure assembled, an experimental set up had to be made. Within the scope of

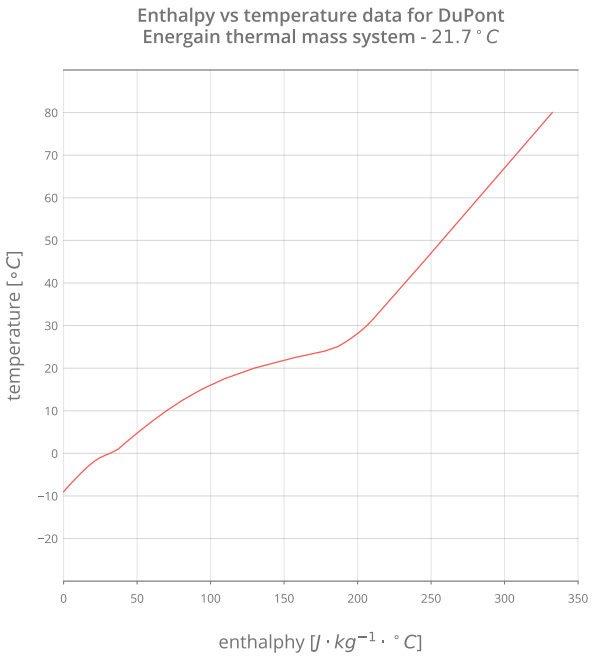

Figure 4: Enthalpy vs temperature data for DuPont Energain PCM [14].

Figure 5: Final wooden structure without PCM boards.

(a) Wooden structure with PCM boards (1/3).

(b) Wooden structure with PCM boards (2/3).

(c) Wooden structure with PCM boards (3/3).

Figure 6: Wooden structure with PCM boards.

this master thesis, twenty four type T thermocouples were manufactured and distributed through the geometric, upper and lower center of each surface, outside the container, suspended in the ceiling and divided into PCM boards' surfaces. These thermocouples can measure temperatures from $-270°C$ to $370°C$ with an accuracy of $\pm 0.5°C$. Data measured by this thermocouples was logged into two *Omega DaqPro* 5300 and one *National Instruments*

NI cDaq 9172. The calibration was done using a *Newport True RMS Supermeter* judiciously following data loggers instructions and verified by a *Fluke TiR27* infrared camera. In addition to this sensors, a temperature and relative humidity data logger (*Hobo* $U10-003$) was also installed in the wooden structure, in order to measure these variables inside the shipping container. This data logger can measure temperatures and relative humidity within the ranges of $-20°C$ to $70°C$ and 25% to 95% with an accuracy of $\pm 0.53°C$ (from $0°C$ to $50°C$) and $\pm 3.5\%$ (from 25% to 85% and from $15°C$ to $45°C$) or $\pm 5\%$ (from 25% to 95% and from $5°C$ to $55°C$), respectively.

For the purpose of measuring outside weather variables, such as dry-bulb temperature, dew point temperature, relative humidity, average wind speed and wind direction, pressure, solar radiation and solar energy, data gathered by a *Davis Instruments Vantage Pro2* weather station installed at Instituto Superior Técnico (Taguspark campus) was used.

Experimental tests lasted three weeks from the 2^{nd} to the 24^{th} of August 2018. Data was saved into data loggers at a minute rate after a three sample average. Experiments were performed with and without PCM boards, with and without night ventilation in the shipping container.

2.3. Modelling and simulation

This problem was modelled using *EnergyPlus*®software, complemented by *SketchUp Pro*® and *Open Studio*®. The final geometry can be seen in figure 7.

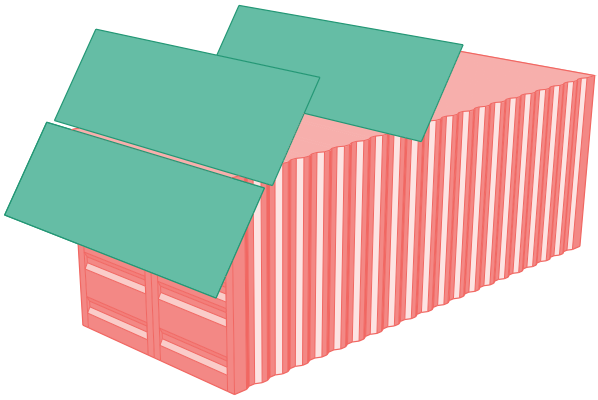

Figure 7: SketchUp model of the shipping container.

For the purpose of modelling PCM materials in *EnergyPlus*®, a conduction finite difference (CondFD) solution algorithm must be added to heat balance equations and conduction transfer functions (CTF) solution algorithm. The two available schemes are Crank-Nicholson (second-order in time semi-implicit scheme) and fully implicit (first-order in time scheme). According to Ozdenefe et al. [15], the fully implicit scheme is more stable over time when modelling PCM and, for this reason, it will be the scheme implemented in this work's simulations. Iterating by fully implicit scheme (Eq. 4) implies to use node temperature of the node being modelled, T_i, node temperature of the adjacent node (exterior of construction), T_{i-1}, node temperature of the adjacent node (interior of construction), T_{i+1}, node temperature in the previous time step, T^j, node temperature in current time step, T^{j+1}, time step, Δt, finite difference layer thickness, Δx, specific heat of the material, C_p, thermal conductivity for interface between i and $i+1$ nodes, k_W, thermal conductivity for interface between i and $i-1$ nodes, k_E, and volumetric mass density, ρ.

$$C_p \rho \Delta x \frac{T_i^{j+1} - T_i^j}{\Delta t} = k_W \frac{T_{i+1}^{j+1} - T_i^{j+1}}{\Delta x} + k_E \frac{T_{i-1}^{j+1} - T_i^{j+1}}{\Delta x} \tag{4}$$

To solve the previous equation, another equation must be added to account for enthalpy vs temperature values inputted by the user (Eq. 5).

$$h_i = HFT(T_i) \tag{5}$$

The finite difference layer thickness, Δx, can be computed knowing the thermal diffusivity of a material, α, the calculation time step, Δt, and a space discretization constant, C, which has a default value of 3 (Eq. 6).

$$\Delta x = \sqrt{C \alpha \Delta t} \tag{6}$$

When PCM are being simulated, a third equation (Eq. 7) must be added in order update specific heat values for each iteration, using enthalpy-temperature data inputted by the user.

$$C_p = \frac{h_i^{j+1} - h_i^j}{T_i^{j+1} - T_i^j} \tag{7}$$

Finally, if a variable thermal conductivity material is specified, its thermal conductivity must be updated as well, using equations 8 and 9:

$$k_W = \frac{k_{i+1}^{j+1} - k_i^{j+1}}{2} \tag{8}$$

$$k_E = \frac{k_{i-1}^{j+1} - k_i^{j+1}}{2} \tag{9}$$

In agreement with this numerical information and after running some test simulations, it was set a time step of 3 minutes and a 1 node spacing grid. These values are within the desirable range suggested in previous studies [14].

To run the *EnergyPlus*® model, two weather files were used: a *epw* file which gathers Lisbon's real weather data from the year of 2005 and a file with real measured data.

PCM boards were modelled as internal mass. Thus, *MaterialProperty:PhaseChange* and *MaterialProperty:VariableThermalConductivity* *EnergyPlus*® objects were filled with the respective enthalpy vs temperature curves and thermal conductivity for the different phases. Besides the real *DuPont Energain*® with a melting point of $21.7°C$, more five boards with melting point values of $19.7°C$, $23.7°C$, $25.7°C$ and $29.7°C$ were simulated.

Internal gains were also taken into account. In this sense, two distinctive scenarios were modelled: (a) experimental scenario and (b) a virtual office. In the experimental scenario, only some appliances from the photovoltaic system and a lead battery were considered inside the container, which were continuously on. In the virtual office scenario, in addition to the previous equipment, a $20\,W$ light bulb and a person were supposed between $9\,a.m.-12\,a.m.$ and $1\,pm.-6\,p.m.$.

Furthermore, two types of ventilation were assumed inside the container such as natural ventilation and mechanical ventilation. Natural ventilation was obtained by equation 10, knowing the average value of wind speed, v, the smallest opening area, A, and the room volume, V, which gives an inside air renovation of 5.268 air changes per hour (ACH).

$$ACH = \frac{0.65 \times v \times A \times 3600}{V} \tag{10}$$

On the other hand, mechanical ventilation was given by a fan installed inside the container. Although this fan had a maximum air room renovation of $21.1\,ACH$, three extra scenarios were also simulated: $0\,ACH$, $5\,ACH$, $10\,ACH$.

Moreover and in order to obtain the effect that incorporating PCM into the shipping container can trigger, a theoretical heat, ventilation and air conditioning (HVAC) system was designed. This system was a unitary system constituted by a $300\,Pa$ blow-through fan complemented by heating and cooling coils. This system had a cooling and a heating coefficient of performance (COP) of 5 and 3, respectively, and the schematic representation can be seen in figure 8.

This system was setted to answer a heating set point of $18°C$ and a cooling point of $27°C$. These values were obtained using the ASHRAE Standard $55-2017$ Thermal Comfort model, which computed Winter and Summer thermal comfort zones (Fig. 9). In this model a 61% relative humidity, a $25°C$ mean radiant temperature, a $0.1\,m\cdot s^{-1}$ air speed, a metabolic rate of 1.1 (reading, writing) and clothing levels of 1.0 (Summer) and 0.5 (Winter) were assumed.

Electricity costs for cooling and heating demands of the HVAC system installed in the container was one of the desired outputs. In this sense, electricity tariffs were added to the model using an electricity bill's data and the *UtilityCost:Tariff* and *Schedule:Compact* *EnergyPlus*® objects.

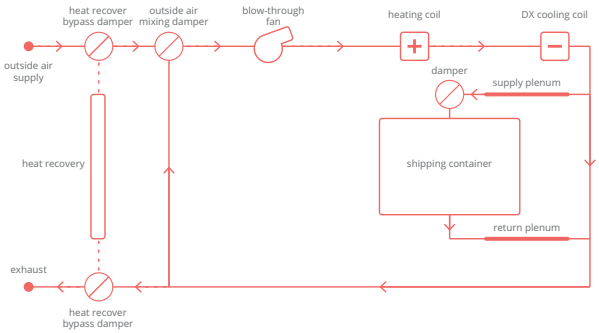

Figure 8: Schematic representation of the unitary HVAC system modelled.

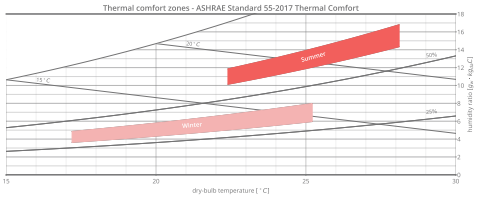

Figure 9: ASHRAE thermal comfort zones for Winter and Summer.

3. Results

3.1. Model validation

To validate the *EnergyPlus*® model described in section 2.3, measured and predicted temperatures were compared.

Experimental tests without PCM took place from the 8^{th} to the 10^{th} of August, 2018. During this period, the model registered a maximum temperatures difference between real and simulated data or maximum error (ME) of $4.89°C$, a mean average error (MAE) of $1.00°C$ and a root mean square error (RMSE) of $1.50°C$. Provided that temperatures sensor had an uncertainty of $\pm 0.53°C$, it can be concluded that the magnitude of the perceived errors were acceptable. Furthermore, the model validation equations 2 and 3 computed a NMBE of 1.9% and a CVRMSE of 6.65%, which fell inside the suitable limits. Therefore, the *EnergyPlus*® model without PCM was validated (Tab. 1).

Table 1: Errors and validation indices for model validation without PCM boards.

temperatures				
ME ($°C$)	MAE ($°C$)	RMSE ($°C$)	NMBE (%)	CVRMSE (%)
4.89	1.00	1.50	1.90	6.65

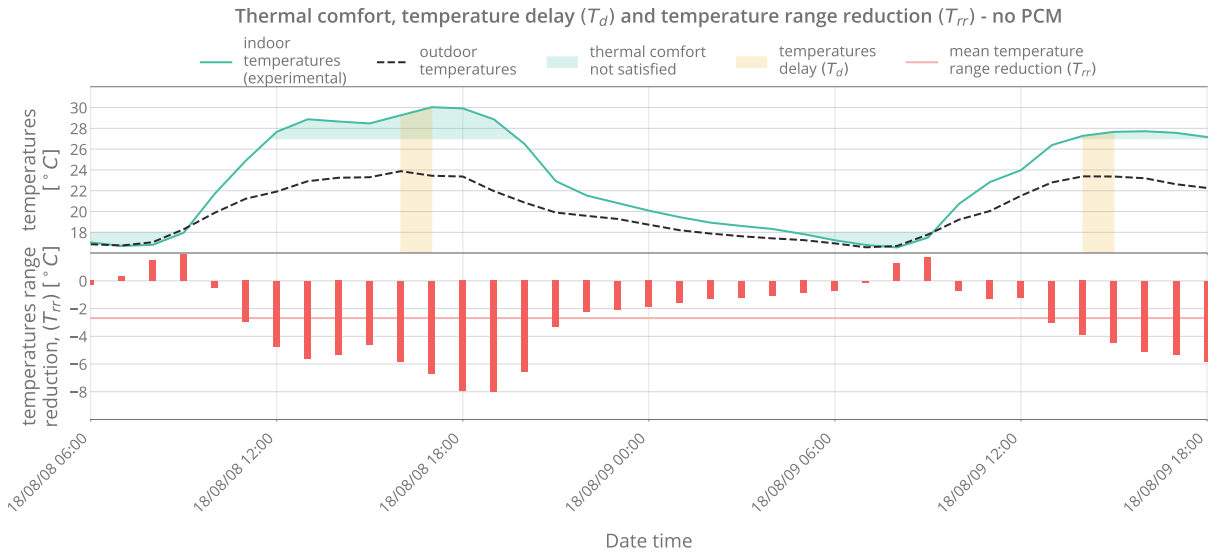

Figure 10: Thermal comfort, temperature delay (T_d) and temperature range reduction (T_{rr}). Experimental data measured without PCM.

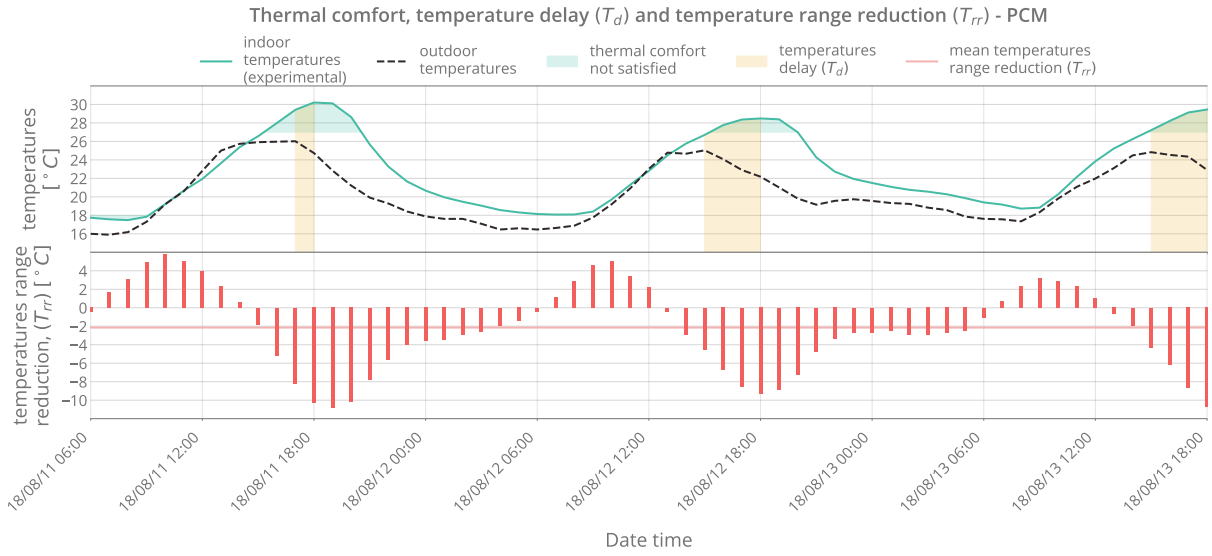

Figure 11: Thermal comfort, temperature delay (T_d) and temperature range reduction (T_{rr}). Experimental data measured with thirty PCM panels.

Besides temperatures, relative humidity was also compared. Measured and predicted data had a ME of 16.56%, a MAE of 6.62% and a RMSE of 7.69%, which were admissible taking into account a measurement uncertainty of ±3.50%.

On the other hand, experimental tests with PCM took place from the 11^{th} to the 14^{th} of August, 2018. The ME recorded was $3.21°C$, whereas the MAE and the RMSE were $1.40°C$ and $1.58°C$, respectively. Model validation equations estimated a NMBE and a CVRMSE of 2.08% and 6.93%, thus the *EnergyPlus*® model with PCM was validated (Tab. 2).

Table 2: Errors and validation indices for model validation with PCM boards.

temperatures				
ME (°C)	MAE (°C)	RMSE (°C)	NMBE (%)	CVRMSE (%)
3.21	1.40	1.58	2.08	6.93

Measured and predicted relative humidity provided a ME of 14.93%, a MAE of 7.22% and a RMSE of 8.53%.

3.2. Effect of PCM in thermal inertia and comfort

The figure 10 shows outdoor and experimental indoor temperatures measured during tests without

PCM. It can be seen that indoor temperatures are in average higher ($2.69°C$) than the outside temperatures and this difference rises with temperatures increase. However, for colder periods, indoor temperatures occasionally fall down the outdoor temperatures. This means that, since the container has a low thermal inertia enclosure, it works as an amplifier of the external climate. In this sense, thermal discomfort was felt during 11 hours over the two experimental days (44%). Moreover, indoor temperatures were one hour late in respect to outdoor temperatures.

On the other hand, this scenario was relatively different over experiments with PCM (Fig. 11). This time indoor temperatures were in average $2.14°C$ higher than outside temperatures. However, looking to the figure at colder periods, it can be clearly noticed that now indoor temperatures did not fall below the outdoor ones. Provided that, thermal discomfort were only felt during 14 hours over the three experimental days (19%) and, indoor temperatures suffered a three hour delay in regard to outside temperatures.

Comparing these experiments, it can be concluded that although average temperatures range reduction, T_{rr}, did not experienced a large progress ($0.55°C$), minimum indoor temperatures and temperatures delay, T_d, demonstrated that PCM boards were effective on improving thermal inertia and thermal comfort. Temperatures delay expanded from one to three hours due to PCM boards. This was thanks to the heat storage capacity of PCM boards that could absorb heat for two hours and, thus, delay peak temperatures over the same time period. At the same time, minimum indoor temperatures never fell down the outside temperatures by virtue of latent heat that started to be released below the $18°C$. This energy discharge allowed to level out minimum temperatures on PCM solidification point (table 3).

Table 3: A thermal comfort comparison of the shipping container with and without PCM.

temperatures range reduction ($°C$)		thermal discomfort (%)		peak temperatures delay ($hours$)	
no PCM	PCM	no PCM	PCM	no PCM	PCM
-2.69	-2.14	44	19	1	3

3.3. Sensitivity analysis on paraffin melting point

Using *EnergyPlus*® model with the HVAC system, lights and people described in section 2.3, a sensitivity analysis was made on the paraffin melting point. This study considered six values for this parameter ($19.7°C$, $21.7°C$, $23.7°C$, $25.7°C$, $27.7°C$ and $29.7°C$) and a night ventilation of $21.1\,ACH$. The respective HVAC energy demand and respective costs due to PCM incorporation can be seen in table 4.

Table 4: Annual cooling and heating energy demand and costs for different PCM melting points.

variable		paraffin melting point ($°C$)						
		no PCM	20	22	24	26	28	30
cooling	demand (MWh)	18.49	17.89	17.92	17.94	17.95	17.95	17.95
	costs (€)	1923.79	1861.16	1863.36	1865.39	1866.48	1867.02	1866.50
heating	demand (MWh)	0.001	0.006	0.006	0.006	0.005	0.005	0.005
	costs (€)	0.05	0.62	0.61	0.58	0.57	0.57	0.55
ventilation	demand (MWh)	0.108	0.108	0.108	0.108	0.108	0.108	0.005
	costs (€)	8.37	8.37	8.37	8.37	8.37	8.37	8.37
total	demand (MWh)	18.60	18.00	18.03	18.05	18.06	18.06	18.06
	costs (€)	1932.21	1870.15	1872.34	1874.34	1875.42	1875.96	1875.42

Installing thirty PCM boards as internal mass, whatever their melting point is, translates into a HVAC energy demand decrease. However, when we look at cooling and heating energy needs, the higher the paraffin melting point, the higher the cooling energy demand and the lower the heating needs of the HVAC unit. Nevertheless, heating needs are despicable in magnitude when compared to cooling.

The same trend can be described in terms of electricity costs both for cooling and heating. In this sense, from those, the best scenario is the one that saves more energy and thus more money per year that is using PCM boards with a $19.7°C$ paraffin melting point. This PCM boards saves around $591\,kWh$ and 62.06€.

3.4. Sensitivity analysis on night ventilation

In this simulation study, thirty PCM boards with a melting point of $19.7°C$ were installed inside the container. The virtual HVAC unit as well as lights and people were also considered to test five different values of night ventilation airflow ($0\,ACH$, $5\,ACH$, $10\,ACH$, $15\,ACH$ and $21.1\,ACH$). HVAC energy needs and costs for simulations with and without PCM boards can be seen in table 5.

Table 5: Annual total energy demand savings and costs savings for rate levels of night ventilation.

total		paraffin melting point ($°C$)				
		0	5	10	15	21.1
no PCM	demand (MWh)	18.58	18.58	18.57	18.59	18.60
	costs (€)	1933.09	1931.58	1931.14	1931.32	1932.21
PCM	demand (MWh)	18.13	18.09	18.04	18.03	18.01
	costs (€)	1885.83	1879.34	1874.98	1872.19	1870.15

The results show that having night ventilation forcing outside intake air decreases energy needs by the HVAC system and the higher the air changes per hour the ventilation provides, the higher the energy improvement. Moreover, comparing results with and without PCM, it can be noticed that night ventilation enhances PCM boards effectiveness by

decreasing HVAC energy needs. Therefore, the best scenario is found when thirty PCM boards with a melting point of 19.7°C and a 21.1 ACH are set, causing savings around 591 kWh and 62.06€.

3.5. Sensitivity analysis on PCM quantity

A parametric study on the PCM quantity was also made, studying the effect that having 0, 6, 12, 18, 24, 30, 36, 42, 48 and 100 PCM boards would have on HVAC energy demand. These boards have a 19.7°C melting point and a 21.1 ACH night ventilation was used (subs. 3.4). Table 6 shows these results.

Table 6: Annual cooling and heating energy demand and costs for different number of PCM boards.

variable		number of PCM panels							
		0	12	24	30	36	42	48	100
total	demand (MWh)	18.60	18.34	18.11	18.01	17.91	17.81	17.72	17.06
	costs (€)	1932.21	1905.49	1881.39	1870.15	1859.43	1849.19	1839.43	1770.01

The HVAC energy demand falls with the increase of the number of PCM boards installed inside the container. This is an expected result because adding PCM units means that were being added heat storage capacity to the container and, therefore, its thermal inertia were being increased. Electricity costs followed the same pattern and thus the most suitable scenario was using 48 boards. It is interesting to look to the test with 100 boards, since it shows that incorporating this amount of boards inside a shipping container twice the size and the same energy HVAC unit, continues to induce an improvement.

3.6. Sensitivity analysis on PCM location

A study on the amount of PCM boards were also done. Eight scenarios were tested: no PCM boards (#1), six internal mass PCM boards (#2), six PCM boards in South sided-door (#3), twelve internal mass PCM boards (#4), twelve PCM boards in floor (#5) and ceiling (#6), thirteen internal mass PCM boards (#7) and thirteen PCM boards in the West sided-wall (#8). The PCM boards had a melting point of 19.7°C.

Table 7: Annual cooling and heating energy demand and costs when PCM boards are located in different places.

variable		number of PCM panels							
		#1	#2	#3	#4	#5	#6	#7	#8
total	demand (MWh)	18.60	18.47	18.60	18.34	18.76	18.64	18.32	18.56
	costs (€)	1932.21	1918.48	1932.32	1905.49	1949.23	1936.44	1903.39	1928.62

From table 7, it can be seen that installing PCM boards as internal mass was the best approach. This was due to that fact that using this configuration allowed to benefit not only from air stratification but also from the cold outdoor intake air that night ventilation's fan used to help on latent heat stored release. It can also be noticed that installing PCM boards in floor or in ceiling worsen energy and costs savings.

3.7. Sensitivity analysis on PCM boards thickness

Finally, the last sensitivity analysis on PCM boards planned to study the effect their thickness had on the HVAC system energy needs and costs. Boards had a melting point of 19.7°C and it was setted a night ventilation of 21.1 ACH. Lights and people inside the container were also considered.

Table 8: Annual cooling and heating energy demand and costs for PCM boards with different thicknesses.

variable		PCM boards thickness (mm)						
		no PCM	5	10	20	30	40	50
total	demand (MWh)	18.60	17.72	17.52	17.18	17.02	16.96	16.94
	costs (€)	1932.21	1839.43	1817.77	1781.49	1764.97	1758.85	1757.51

Table 8 shows that the HVAC energy demand decreases over boards' thickness. However, the rate at which this fall happened was itself diminishing. This occurred for the simple reason that, from a certain thickness baseline, the thickness value was too high to let latent heat access its inner layer. Consequently, having too thick boards did not translate into a proportional energy saving. In this sense, the best option in this study was to use boards with a thickness of 10 mm.

3.8. Economic analysis

For the purpose of understanding if these boards are a good investment, a simple economic analysis based on their payback period was formulated.

Two different scenarios were examined: the experimental setting and the optimal setting obtained by the previous sensitivity analysis. The payback period was computed using the net present value, NPV, concept. The NPV is equal to the sum of the initial investment, I_0, and the present value, PV, which depends on the future cash-flows, C, their inflation rate, g, and the respective rate of return, r, over t years.

$$NPV = I_0 + PV = I_0 + \frac{C}{r-g} - \frac{C}{r-g}\left(\frac{1+g}{1+r}\right)^t \quad (11)$$

This study considered two distinct initial investments: one using the current boards cost (prototype) [16] and the other using a boards cost based on their components market price (estimated) [17–20]. This gave an initial investment output for experimental and ideal prototype of 1358.00€ and

4339.20€, while the initial investment for experimental and ideal estimated scenarios were 231.25€ and 797.63€.

The rate of return, r, was 5.27%, whereas inflation rate of consumer price in electricity sector, g, was 3.19%, being both values based on portuguese data over the last ten years. Cash-flows were HVAC electricity costs savings due to the incorporation of PCM panels inside the container and were 59.87€ and 114.54€ for experimental and ideal scenarios. In this sense, the resulting calculations gave a payback period of thirty two and seventy eight years for experimental and ideal prototype scenarios and five and eight years for experimental and ideal estimated scenarios. Thereby, although the current price does not allow to invest in these PCM boards as a profitable project, in a few years, with a market price reduction, PCM will be a cost-effective investment.

4. Conclusions

This work demonstrated that *DuPont Energain*® thermal mass units are an effective cooling system, suitable for warmer climates. These boards proved to be a thermal inertia supplement capable of delaying maximum temperatures by three hours, which resulted as thermal comfort improvement in terms of time by 25%.

Nevertheless, choosing an appropriate PCM can depend on the climate, the location, PCM thickness, PCM quantity and PCM melting point. Moreover, if available, night ventilation could boost PCM latent heat stored during night, improving the effectiveness of these materials.

Furthermore, despite the fact that these boards do not make a good investment given their current market price, in the future with a massive production of these units, this prospect can change favourably.

Acknowledgements

First and foremost, I have to thank my parents Maria Irene and Duarte Drumond for their love and support throughout my life. Thank you both for being caring and teaching me the values of life. My sister Rita deserves my wholehearted thanks as well.

I would like to sincerely thank my thesis advisers, Dr. Rui Costa Neto and Dr. Laura Aelenei, for their continued guidance and precious advices in the course of this thesis. Their patience and encouragement were vital to me.

My gratitude extends as well to Prof. João Gomes Ferreira for borrowing his infrared camera (*Fluke TiR27*), to Engineer Ricardo Gomes for his time devoted to teach me some basics on *EnergyPlus*® and *P*rof. Carlos Silva for funding this thesis consumables.

To my dear friend António Jacques, thank you for this journey which has lasted since we were five years old and will certainly extend for many years to come.

One last thank you to Gonçalo Silva, the best companionship I could have had during these last months.

References

[1] Ürge-Vorsatz, D., Cabeza, L. F., Serrano, S., Barreneche, C., and Petrichenko, K. "Heating and cooling energy trends and drivers in buildings". *Renewable and Sustainable Energy Reviews* 41 (2015), pages 85–98. DOI: 10.1016/j.rser.2014.08.039.

[2] Lane, G. *Solar heat storage: Latent heat materials*. 1st edition. Volume 1. Jan. 1983.

[3] Soares, N., Costa, J. J., Gaspar, A. R., and Santos, P. "Review of passive PCM latent heat thermal energy storage systems towards buildings' energy efficiency". *Energy and buildings* 59 (2013), pages 82–103. DOI: 10.1016/j.enbuild.2012.12.042.

[4] Akeiber, H., Nejat, P., Majid, M. Z. A., Wahid, M. A., Jomehzadeh, F., Famileh, I. Z., Calautit, J. K., Hughes, B. R., and Zaki, S. A. "A review on phase change material (PCM) for sustainable passive cooling in building envelopes". *Renewable and Sustainable Energy Reviews* 60 (2016), pages 1470–1497. DOI: 10.1016/j.rser.2016.03.036.

[5] Jankowski, N. R. and McCluskey, F. P. "A review of phase change materials for vehicle component thermal buffering". *Applied Energy* 113 (2014), pages 1525–1561. DOI: 10.1016/j.apenergy.2013.08.026.

[6] Hawes, D., Feldman, D., and Banu, D. "Latent heat storage in building materials". *Energy and buildings* 20.1 (1993), pages 77–86. DOI: 10.1016/0378-7788(93)90040-2.

[7] Jacob, R. and Bruno, F. "Review on shell materials used in the encapsulation of phase change materials for high temperature thermal energy storage". *Renewable and Sustainable Energy Reviews* 48 (2015), pages 79–87. DOI: 10.1016/j.rser.2015.03.038.

[8] Soares, N., Gaspar, A., Santos, P., and Costa, J. "Multi-dimensional optimization of the incorporation of PCM-drywalls in lightweight steel-framed residential buildings in different climates". *Energy and buildings* 70 (2014), pages 411–421. DOI: 10.1016/j.enbuild.2013.11.072.

[9] Zhou, D., Tian, Y., Qu, Y., and Chen, Y. "Thermal analysis of phase change material board (PCMB) under weather conditions in the summer". *Applied Thermal Engineering* 99

(2016), pages 690–702. DOI: 10.1016/j.applthermaleng.2016.01.121.

[10] Soares, N., Reinhart, C. F., and Hajiah, A. "Simulation-based analysis of the use of PCM-wallboards to reduce cooling energy demand and peak-loads in low-rise residential heavyweight buildings in Kuwait". *Building Simulation*. Volume 10. 4. Springer. 2017, pages 481–495.

[11] Devaux, P. and Farid, M. M. "Benefits of PCM underfloor heating with PCM wallboards for space heating in winter". *Applied energy* 191 (2017), pages 593–602. DOI: 10.1016/j.apenergy.2017.01.060.

[12] Yang, C., Susman, G., and Dowson, M. "EnergyPlus model of novel PCM cooling system validated with installed system data". *Proceedings of SimBuild* 6.1 (2016).

[13] Peel, M. C., Finlayson, B. L., and McMahon, T. A. "Updated world map of the Köppen-Geiger climate classification". *Hydrology and earth system sciences discussions* 4.2 (2007), pages 439–473. DOI: 10.5194/hess-11-1633-2007.

[14] Tabares-Velasco, P. C., Christensen, C., and Bianchi, M. "Verification and validation of EnergyPlus phase change material model for opaque wall assemblies". *Building and Environment* 54 (2012), pages 186–196. DOI: 10.1016/j.buildenv.2012.02.019.

[15] Ozdenefe, M. and Dewsbury, J. "Thermal performance of a typical residential Cyprus building with phase change materials". *Building Services Engineering Research and Technology* 37.1 (2016), pages 85–102. DOI: 10.1177/0143624415603004.

[16] *Phase Change Materials: And the Arup thermal calculator. Robert Matthews SelfBuild site.* 2018. URL: https://irp-cdn.multiscreensite.com/e3960383/files/uploaded/2014%20K%20Phase%20change%20materials.pdf (visited on 07/11/2018).

[17] *Polyethylene Glycol 200 (PEG 200). Alibaba site.* 2018. URL: https://www.alibaba.com/product-detail/Factory-price-PEG-200-400-600_60251067131.html?spm=a2700.7724838.2017115.97.16dd6e71GjHGPB (visited on 09/14/2018).

[18] *Alloy 8011. Alibaba site.* 2018. URL: https://www.alibaba.com/product-detail/2018-Hotsale-Aluminum-Foil-Jumbo-Roll_1613063452.html?spm=a2700.7724857.normalList.1.344c690eKR9Nrs (visited on 09/14/2018).

[19] *N-heptadecane, paraffin wax. Alibaba site.* 2018. URL: https://www.alibaba.com/product-detail/high-quality-best-price-629-78_60746572829.html?spm=a2700.7724838.2017115.30.316db5e52ZtRNv (visited on 09/14/2018).

[20] *Polyethylene Glycol 600 (PEG 600). Alibaba site.* 2018. URL: https://www.alibaba.com/product-detail/Factory-price-PEG-200-400-600_60251067131.html?spm=a2700.7724838.2017115.51.52383747Zbg4tT (visited on 09/14/2018).